Surface relief grating growth in thin films of mexylaminotriazine-functionalized glass-forming azobenzene derivatives

Othmane R. Bennani,[a,b] Tayel A. Al-Hujran,[c] Jean-Michel Nunzi,[a] Ribal Georges Sabat[b] and Olivier Lebel*[c]

Received (in XXX, XXX) Xth XXXXXXXXX 200X, Accepted Xth XXXXXXXXX 200X
First published on the web Xth XXXXXXXXX 200X
DOI: 10.1039/b00000000x

Azobenzene-containing materials exhibit various photomechanical properties, including the formation of surface relief gratings (SRG) when irradiated with two interfering laser beams. In a recent study, a novel glass-forming derivative of Disperse Red 1 (DR1) with a mexylaminotriazine group was synthesized in high yield with a simple and efficient procedure, and showed the ability to form high-quality amorphous thin films with a high resistance to crystallization. Irradiation of films of this material yielded SRG with growth rates comparable to other reported azo materials. Herein, a series of closely related molecular glasses containing azobenzene chromophores with various absorption maxima ranging from 410 to 570 nm were synthesized, and their physical and photomechanical properties were studied. All materials studied showed the ability to form stable glassy phases, and irradiation with lasers emitting at various wavelengths allowed to perform a comparative study of SRG growth within a series of analogous chromophores.

Introduction

The *cis-trans* isomerisation of azobenzene and its derivatives upon irradiation with visible light is a well-documented phenomenon.[1] Typically, azobenzene derivatives can rapidly isomerize back and forth between both forms, which, when occurring in the solid state, leads to migration at the molecular level due to the motion of the azo groups, eventually leading to photomechanical phenomena, including the formation of surface relief gratings (SRG).[2-4] SRG typically occur when a material containing azobenzene moieties is irradiated with two interfering coherent laser beams, upon which the molecular motion causes the formation of peaks and troughs in the surface of the material which mimic the interference pattern.[5] Several applications have been proposed for SRG, including resonant waveguide filters,[6] plasmonic biosensors,[7] DNA-tunable dye laser,[8] organic light emitting diodes,[9] light-harvesting structures for photovoltaic cells,[10-11] as well as many other applications.[12]

As most simple azobenzene derivatives readily crystallize, studies of their photophysical behavior in the solid state use materials where the chromophores are either dispersed in or bonded to polymers,[1,13-14] or incorporated into small molecules that can readily form glassy phases.[15-17] The latter class of materials, called molecular glasses or amorphous molecular materials, possesses several advantages over polymers linked to their smaller size and monodisperse nature, which ensures that samples are homogeneous and constituted of a single, pure component.[18-19] Not only does this make purification and characterization easier, it also increases the reproducibility of their behavior. On the other hand, small molecules tend to crystallize more easily, but with careful molecular design it is possible to generate molecular glasses that do not crystallize under ambient conditions.[20-23] Generally, small molecules that possess an irregular and non-planar shape, can adopt different conformations, and interact weakly and indiscriminately with neighboring molecules show a higher propensity to form glassy phases.[20] While most azobenzene derivatives tend to crystallize, the presence of bulky bis(9,9-dimethylfluorenyl)amino,[15] bis(4-biphenyl)amino,[16] or triphenylmethyl[17] groups on azo chromophores slows down crystallization kinetics enough to allow the compounds to be isolated in glassy form.

Mexylaminotriazines are one family of molecular glasses that, despite defying some of the traditional structural features shared by other molecular glasses, shows extreme resistance to crystallization.[24] Unlike classic molecular glasses, mexylaminotriazines show relatively small size, higher symmetry, relatively rigid structures, and the potential to self-assemble along pairs of hydrogen bonds. Instead, these compounds resist crystallization because of hindered conformational equilibria that limits packing in an ordered fashion, and hydrogen bonding to help slow their crystallization kinetics by reducing their mobility in the solid state.[25] Derivatives incorporating various structural elements can be easily synthesized from cyanuric chloride, 3,5-dimethylaniline and other amines.[26] By varying the amino substituents, it is possible to control the physical properties of the materials (solubility, glass transition temperature (T_g), etc.), and it is possible to introduce reactive functional groups that can be used to anchor other functional compounds, including chromophores.[27] This modular approach allows the design and synthesis of novel glass-forming materials in an efficient fashion, with high yields, and with minimal screening.

Materials containing several azobenzene chromophores with

various absorption ranges, polarity, and steric bulk have been studied so far, but in most cases, with different polymer backbones or small-molecule structures.[1,13-14] Comparisons between different chromophores are complicated by differences in their molecular structures that extend beyond the chromophore. Furthermore, while azobenzene chromophores with absorptions between 400 and 500 nm have been extensively studied,[2-5] azobenzene derivatives can be synthesized with absorption ranges higher than 700 nm,[28] and few studies exist on the photomechanical properties of azobenzene chromophores with absorption maxima over 500 nm.[3,29-31]

A previous report introduced a mexylaminotriazine derivative of Disperse Red 1 (**1**), which could be easily prepared in yields over 90% and that showed to be capable of readily forming amorphous thin films which could yield surface relief gratings (SRGs) upon irradiation.[32] In the present work, the same synthetic strategy was used to generate mexylaminotriazine glasses functionalized with various azo chromophores with a wide range of absorption maxima spanning 410 to 570 nm. Their photomechanical behavior was studied using different lasers, and it was shown that while most materials studied showed the capability to inscribe SRGs with a rate loosely proportional to their absorbance with the corresponding lasers, azothiazole-based chromophores showed very slow SRG growth, even at wavelengths near their absorption maxima. This behavior is likely due to a slow *cis-trans* isomerisation rate, though it is unclear at this stage if *cis-trans* isomerisation is hindered by an intrinsically high isomerisation barrier, the formation of aggregates in the solid state, or hydrogen bonding in the material.

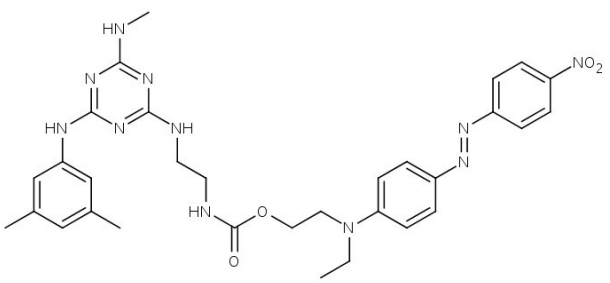

1

Experimental Section

General

4-(N-(2-Hydroxyethyl)-N-ethylamino)azobenzene (**3a**),[33] 4-(N-(2-hydroxyethyl)-N-ethylamino)-3',5'-dichloroazobenzene (**3b**),[34] 4-(N-(2-hydroxyethyl)-N-ethylamino)-4'-phenylazoazobenzene (**3c**),[34] 2-[4-(N-(2-hydroxyethyl)-N-ethylamino)phenylazo]-6-nitrobenzothiazole (**3d**)[35] and 2-[4-(N-(2-hydroxyethyl)-N-ethylamino)phenylazo]-5-nitrothiazole (**3e**)[36] were prepared according to the literature. 2-Methylamino-4-mexylamino-6-(2-aminoethylamino)-1,3,5-triazine (**2**) and Disperse Red 1 glass **1** were purchased from Solaris Chem, Inc., N-ethyl-N-(2-hydroxyethyl)aniline, aniline, 3,5-dichloroaniline, 2-amino-5-nitrothiazole and 2-amino-6-nitrobenzothiazole were purchased from Sigma-Aldrich, 4-aminoazobenzene hydrochloride was purchased from TCI America, N,N'-Carbonyldiimidazole (CDI) was purchased from Oakwood Chemicals, and all solvents were purchased from Caledon Labs. All reagents were used without further purification. Reactions were performed under ambient atmosphere unless otherwise specified. Glass transition temperatures were determined with a TA Instruments 2010 Differential Scanning Calorimeter calibrated with indium at a heating rate of 5 °C/min from 30 to either 150 (for compounds **4d-e**) or 200 °C. Values were reported after an initial heating and cooling cycle as the half-height of the heat capacity change averaged over two heating runs. FTIR spectra were acquired with thin films cast from CH_2Cl_2 on KBr windows using a Perkin-Elmer Spectrum 65 spectrometer. UV-visible absorption spectra were acquired using a Hewlett-Packard 8453 spectrometer. ^{1}H NMR spectra were acquired on either a 400 MHz Bruker AV400 spectrometer at 363 K, while ^{13}C NMR spectra were recorded on a 300 MHz Varian Oxford spectrometer at 298 K.

Synthesis

Synthesis of Azo Glass 4a

To a stirred suspension of N,N'-carbonyldiimidazole (0.729 g, 4.50 mmol) in dry THF (5 mL) in a dry round-bottomed flask equipped with a magnetic stirrer was slowly added a solution of 4-(N-(2-hydroxyethyl)-N-ethylamino)azobenzene (0.876 g, 3.25 mmol) in dry THF (10 mL) at ambient temperature, then the mixture was stirred for 18 h under nitrogen atmosphere. CH_2Cl_2 and H_2O were added, then the layers were separated, and the organic layer was washed two more times with copious amounts of H_2O. The organic extract was recovered, dried over Na_2SO_4, filtered, and the solvent was evaporated. The crude residue was redissolved in THF (20 mL), then 2-methylamino-4-mexylamino-6-(2-aminoethylamino)-1,3,5-triazine (1.00 g, 3.48 mmol) was added and the mixture was refluxed for 18 h. The solvent was evaporated, then 1M aqueous HCl was added, then the precipitated product was collected by filtration and washed with 1M aq. HCl and H_2O until the effluent was colorless. The residue was dissolved in acetone, then CH_2Cl_2 and aq. $NaHCO_3$ were added. The layers were separated, the organic layer was dried over Na_2SO_4, filtered, and the volatiles were thoroughly evaporated under reduced pressure to yield 1.68 g of pure glass **4a** (2.89 mmol, 89%). T_g 63 °C; FTIR (CH_2Cl_2/KBr) 3401, 2973, 2928, 2854, 1701, 1599, 1565, 1515, 1439, 1397, 1359, 1324, 1299, 1255, 1189, 1153, 1137, 1090, 1065, 1039, 840, 809, 767, 736, 689 cm^{-1}; ^{1}H NMR (400 MHz, DMSO-d_6, 363 K) δ 8.28 (br s, 1H), 7.78 (m, 4H), 7.52 (t, ^3J = 7.3 Hz, 2H), 7.41 (t, ^3J = 7.3 Hz, 1H), 7.41 (s, 2H), 6.88 (d, ^3J = 9.1 Hz, 2H), 6.83 (br s, 1H), 6.57 (s, 1H), 6.39 (br s, 1H), 6.31 (br s, 1H), 4.20 (t, ^3J = 5.8 Hz, 2H), 3.64 (t, ^3J = 5.8 Hz, 2H), 3.50 (q, ^3J = 7.1 Hz, 2H), 3.43 (q, ^3J = 5.8 Hz, 2H), 3.26 (q, ^3J = 5.8 Hz, 2H), 2.84 (d, ^3J = 4.5 Hz, 3H), 2.24 (s, 6H), 1.18 (t, ^3J = 7.1 Hz, 3H) ppm; ^{13}C NMR (75 MHz, DMSO-d_6) δ 166.5, 166.1, 164.4, 156.7, 152.9, 150.7, 142.9, 141.0, 137.4, 129.9, 129.6, 125.4, 123.1, 122.2, 117.6, 111.7, 61.5, 49.2, 45.4, 40.4, 40.4, 27.7, 21.7, 12.4 ppm; UV-Vis (CH_2Cl_2): λ_{max} (ε) 413 nm (8 700); HRMS (ESI) m/z: [M + H]$^+$ calcd. for $C_{31}H_{39}N_{10}O_2$: 605.3071, found:

605.3081.

Synthesis of Compounds 4b-4e

Compounds **4b-4e** were synthesized by procedures similar to those used for compound **4a**. Synthetic details can be found in Electronic Supplementary Information (ESI).†

Thin Film Deposition

Solutions of compounds **1** and **4a-e** were prepared at a concentration of 3 wt% in CH_2Cl_2 and mechanically shaken for 1 hour. They were then filtered through a 50-microns syringe filters. Thin films were then prepared by spin-coating using a Headway Research spin-coater: 3 mL of solution was deposited on a 3 x 3 cm^2 BK7 glass slide, followed by spinning at a rate of 1500 rpm for 40 seconds. After deposition, all films of azo glasses **1** and **4a-e** were dried in a Yamato ADP-21 oven at 95 °C for 10 minutes. This procedure yielded uniform films having an average thickness around 400 nm as measured using a Sloan Dektak II D profilometer (model 139961).

Surface Relief Grating Writing

Thin films of azo glasses **1** and **4a-e** were irradiated with two interfering beams from three different laser systems using a Lloyd mirror set-up.[5] The first laser was a 2.5 W Argon-Ion Lexel model 85, which emitted laser lines at 488 nm, 496.5 nm and 514 nm. The irradiance of the other lines of this Argon-Ion laser was too low to inscribe gratings. The second laser used was a 532 nm wavelength Coherent Verdi diode-pumped laser (model 0174-525-52, 5 Watts), and the third laser was a 150 mW Jodon He-Ne laser emitting at 632 nm. The light beam of each laser was collimated and circularly polarized. A variable iris was used to set the laser beam diameter at around 1 cm. The laser irradiance was measured using a Coherent Powermax Wand. The interference pattern by the Lloyd mirror from each laser line resulted in sinusoidal light intensity variations along the vertical axis. Upon exposure to the azo glass films, surface relief gratings in the form of half discs with an area of approximately 1 x 0.5 cm^2 were recorded. The gratings' pitch could be varied by rotating the Lloyd mirror with respect to the writing beam, but for this series of experiments, the pitch was kept constant at 500 nm for all SRGs. The depth of the gratings was dependent on the laser exposure time and irradiance.

The time-dependent diffraction efficiency was monitored in-situ during laser irradiation. A probe low-power He-Ne laser was incident on the portion of the thin film where the SRG was forming. As the grating appeared, the first order diffracted beam from the He-Ne laser was mechanically chopped and then incident on a silicon photodetector. The signal of the photodetector was then measured by a lock-in amplifier and recorded by a computer. The diffraction efficiency was obtained by dividing the signal of the first by the zeroth diffraction order.

Atomic Force Microscopy

AFM scans were performed using an Ambios Q-Scope Atomic Force Micoscope, in tapping mode with a scanning rate of 1 Hz using 40 N/m force constant Quesant Premounted cantilever probes.

Results and Discussion

Synthesis

Azo chromophore-substituted glasses **4a-e** were synthesized by a procedure similar to the one used for Disperse Red 1 derivative **1**[32] from the respective N-ethyl-N-(2-hydroxyethyl)amino azo derivatives **3a-e**[33-36] and amino-functionalized mexylaminotriazine derivative **2** in the presence of N,N'-carbonyldiimidazole (CDI) (Scheme 1). A solution of chromophore in THF was first added to a suspension of CDI in THF at ambient temperature to generate an imidazolylcarbamate intermediate, which was then heated with glass **1** in THF to give adducts **4a-e**. For thiazole-containing dyes **3d-e**, the starting materials and intermediates were much less soluble in THF than azobenzene derivatives **3a-c**, therefore the reaction with CDI was performed in DMF instead of THF, and the imidazolylcarbamate intermediates were isolated by precipitation. Additionally, while azobenzene-based glasses **4a-c** gave very high yields (near 90%), thiazole-containing azo glasses **4d-e** were obtained in 73-74 % yields, as intractable degradation products were also obtained. In the case of 5-nitrothiazolyl derivative **4e**, those impurities could be conveniently removed by dissolving the crude product in dichloromethane. However, for 6-benzothiazolyl analogue **4d**, those impurities were also soluble in dichloromethane, and the product had to be purified by filtration on a short silica pad using $CHCl_3$/acetone 9:1. The identity of the products could be easily confirmed by the appearance of a carbamate C=O band near 1705 cm^{-1} by FTIR spectroscopy, or by the shift of the -CH_2- peak from 2.8 ppm to 3.2 ppm, and the disappearance of the -NH_2 and -OH peaks from both reactants, by ^{1}H NMR spectroscopy.

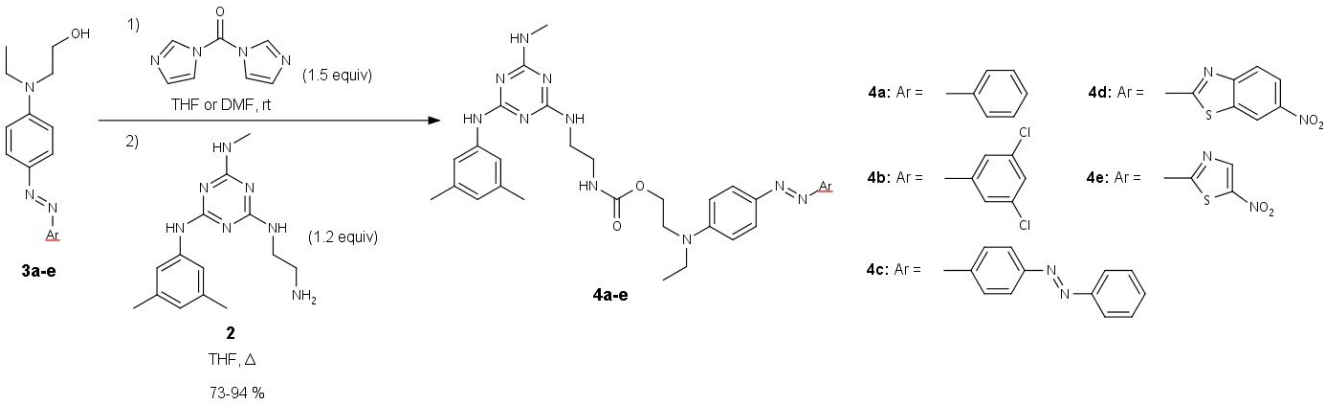

Scheme 1. Synthesis of azo-functionalized glasses **4a-e**.

Physical Properties

As with DR1-substituted analogue **1**, glasses **4a-e** proved capable of readily forming glassy phases with no signs of crystallization upon heating at a rate as slow as 0.5 ºC/min. Compounds **4a-c** were stable up to 200 ºC, while thiazole-substituted derivatives **4d-e** started showing decomposition around 180 and 150 ºC, respectively. DSC scans of compounds **4a-e** are shown in Figure 1, while T_g values are listed in Table 1. DSC scans shown were recorded after an initial heating scan to erase the thermal history of the samples and during which no melting transitions were observed. T_g values are close to the one previously reported for DR1 glass **1** (71 ºC) and showed a slight increase with increasing polarity from 63 ºC for phenyl-substituted dye **4a** to 73 ºC for 6-nitrothiazolyl analogue **4e**. Only bis(azo) derivative **4c** showed a slightly lower T_g value than expected (64 ºC), possibly owing to the higher flexibility of the chromophore. The polarity of the azo chromophore thus impacts the T_g of the material, albeit very slightly compared to substituents on the triazine ring.

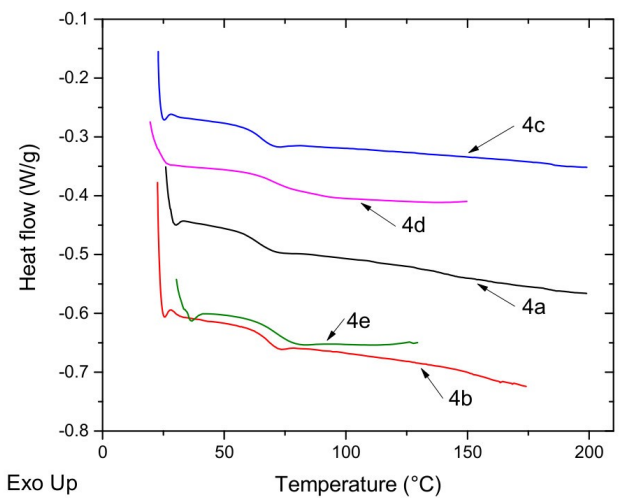

Fig. 1 DSC scans of compounds **4a-e**, recorded at a heating rate of 5 ºC/min after an initial heating scan. T_g are indicated.

Table 1 Glasses transition temperatures (T_g) for azo glasses **4a-e**.

Compound	T_g (ºC)
4a	63
4b	68
4c	64
1[a]	71
4d	72
4e	73

[a] Ref. 32

All five azo glasses reported herein show appreciable solubility in various organic solvents and can be easily processed from solution by spin-coating. The films thusly obtained are high-quality, uniform, and devoid of crystalline imperfections (this was confirmed by the absence of peaks by PXRD). The monodisperse nature of the materials resulted in processing behavior that was consistent and reproducible from one sample to another.

UV-Visible spectra of compounds **4a-e** were recorded both in CH_2Cl_2 solution and as thin films, and the values are reported in Table 2. The absorption maxima for all five compounds are very close to reported values for the precursor dyes (Figure 2a), as was the case for Disperse Red 1-based glass **1**.[32] Absorption maxima for the dyes in thin films were very close (within 9 nm in each case) of their values in solution (Figure 2b). Those shifts are interpreted as the solvatochromic shift expected with the polarity change from the solution (CH_2Cl_2) to the thin film (triazine-glass) environment.

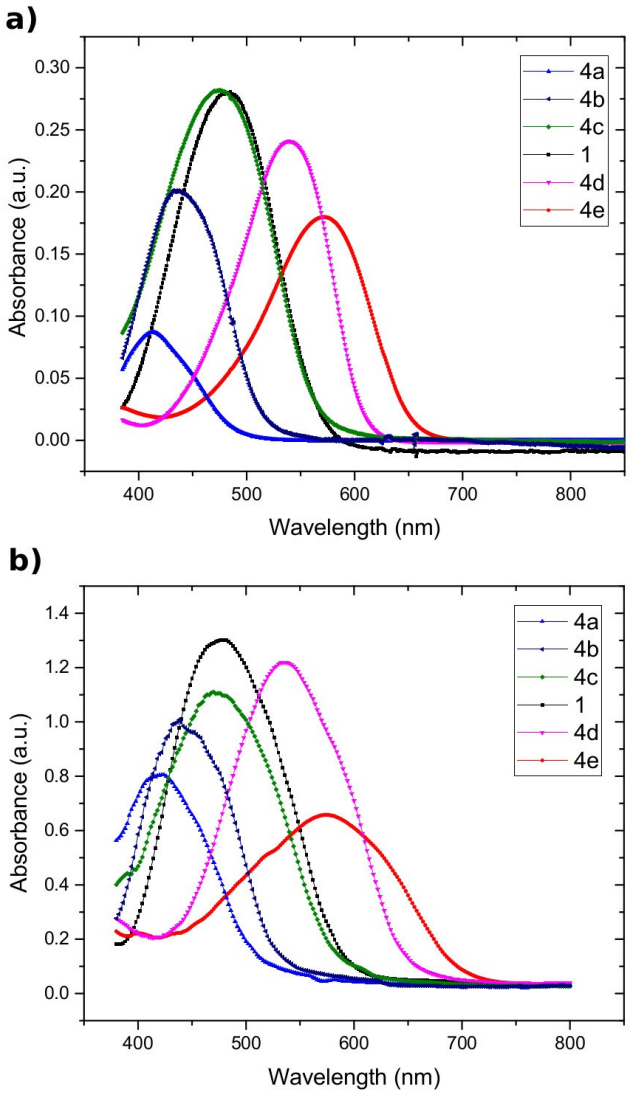

Fig. 2 UV-Visible spectra for azo glasses **1** and **4a-e**, a) in 0.01 mM CH_2Cl_2 solution, and b) as solid thin films.

Table 2 Absorption bands for azo-functionalized glasses **1** and **4a-e** in CH_2Cl_2 solution and as solid thin films.

Compound	λ_{max} (CH_2Cl_2) (nm)	ε (CH_2Cl_2) (cm^{-1} M^{-1})	λ_{max} (film) (nm)
4a	413	8 700	416
4b	435	20 000	432
4c	475	28 000	470
1[a]	485	28 000	476
4d	539	24 000	538
4e	571	18 000	576

[a] Ref. 32

Photomechanical Properties

Surface relief gratings were inscribed on the various thin films as detailed previously. The diffraction efficiency of the gratings is strongly dependent on their depth, hence, indirectly related to the laser exposure time and irradiance. Nonetheless, too much irradiance too quickly can saturate the sample and destroy the gratings, thus reducing the overall diffraction efficiency. In order to provide an accurate comparison between the various compounds, all samples were prepared in an identical manner and the diffraction efficiencies were obtained at the same laser powers. Furthermore, the measurements were conducted on various samples under the same conditions and the results were averaged and compiled in the plots that follow.

The diffraction efficiencies with various Argon-Ion laser lines488, 496.5 and 514 nm) are shown in Figure 3. Diffraction efficiencies are also compiled for every SRG in Table S1 (see ESI).† The 488, 496.5 and 514 nm laser lines had irradiances of 80, 31 and 95 mW/cm^2 respectively. SRGs formed on only azo glasses **1** and **4a-c** at these wavelengths with azo glass **1** being much stronger than the other azo glasses **4a-c** in the 488 nm laser line. The diffraction efficiencies of glasses **4a-c** were proportional to their relative absorptions at the given wavelengths. This is to be expected since azo glass **1** has its absorbance maxima closest to this wavelength. In figure 3b, azo glass **4c** shows the strongest diffraction signal despite having its absorbance maxima around 470 nm. As the inscribing laser wavelength increases, the diffraction signal from azo glasses **4a-b** decreases despite the stronger irradiance at the 514 nm laser line. This is because their absorbance decreases dramatically around 500 nm, as seen in Figure 2. Unexpectedly, there were no SRGs formed in azo glasses **4d-e** at any of the Argon-Ion wavelengths. This behavior cannot be rationalized from absorbance alone, because the molar absorptivity coefficients (ε) of compounds **4d** range between 12000 and 20000 $M^{-1}cm^{-1}$ at the three wavelengths studied, while those of compound **4e** range from 7000 to 10000 $M^{-1}cm^{-1}$. Those values are similar to higher than those for compound **4b** (2300-9500), and orders of magnitude higher than that of compound **4a** (200-1000), which both show SRG growth. A representative Atomic Force Microscopy (AFM) image of a SRG inscribed on compound **4c** with the 488 nm laser line and an exposure time of 240 seconds is shown in Figure 4. It shows a pitch of 750 nm and a grating depth close to 200 nm.

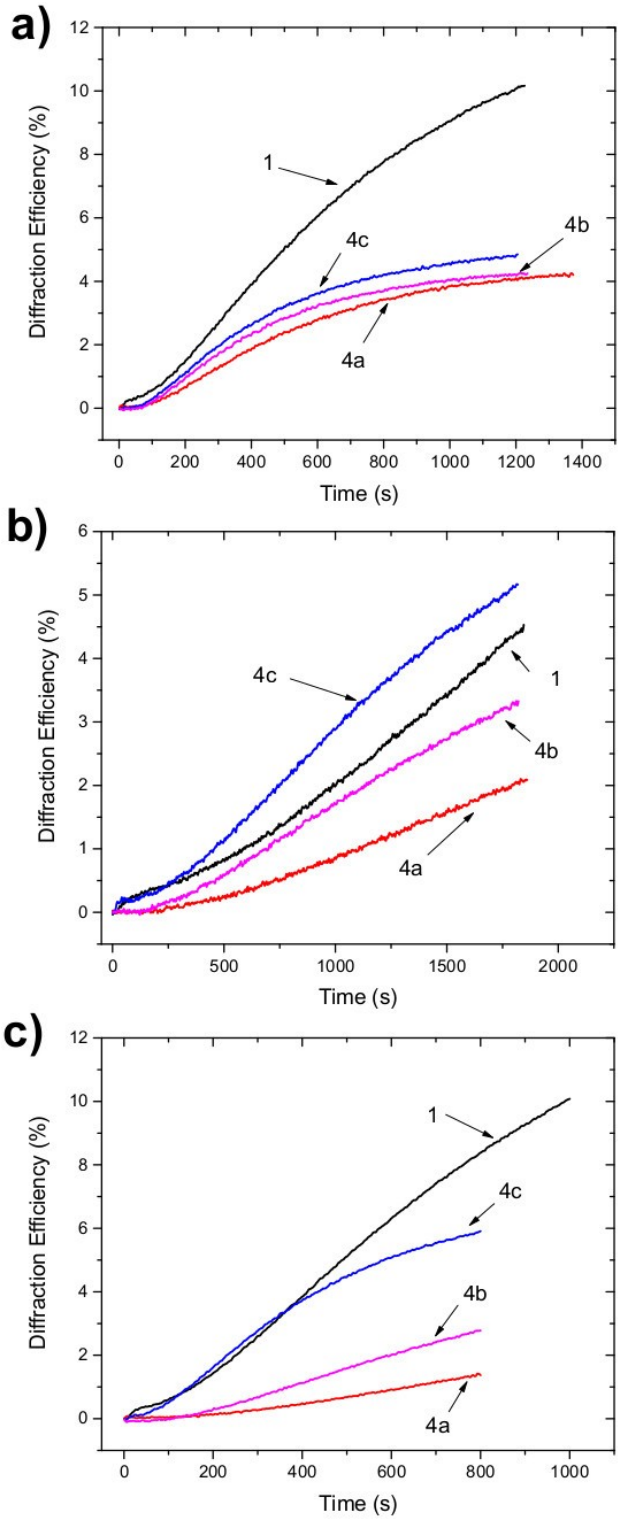

Fig. 3 Diffraction efficiency as a function of exposure time for films of azo glasses **1** and **4a-c** at the wavelengths a) 488 nm, b) 496.5nm, and c) 514 nm.

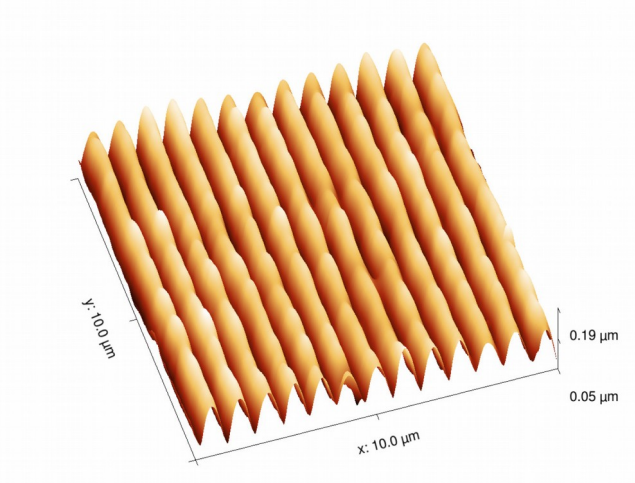

Fig. 4 Atomic Force Microscopy (AFM) scan of a surface relief grating written on a thin film of compound **4c** with an Argon-Ion 488 nm laser line and an exposure time of 240 s. The pitch of the SRG is 750 nm with a 200 nm depth.

The diffraction efficiencies of the SRGs with the 532 nm Coherent diode-pumped green laser at irradiances of 157, 344 and 521 mW/cm^2 are shown in Figure 5 for compounds **1** and **4a-c**, and in Figure 6 for compounds **4d-e**. As diffraction efficiency is correlated linearly with grating depth, SRG heights were measured by AFM for gratings inscribed on compounds **1** and **4a-c** at 532 nm at an irradiance of 344 mW/cm^2 and an exposure time of 300 s. Grating height is plotted as a function of diffraction efficiency in Figure 7. It should be noted that the maximum diffraction efficiencies obtained in this work are different for compound **1** from what has been published earlier by our group.[32] This is because the diffraction efficiency is strongly dependent on the probe laser polarization. Therefore, a different polarization will yield significantly different efficiency values, irrelevant of the SRG depths. Nonetheless, the experimental set-up throughout this work was kept unchanged, so it should provide an accurate comparison between the different compounds presented here. Despite the extremely small absorbance of the azo glasses **4a-b** at 532 nm, there are still SRGs forming, although at low efficiency values. As the laser irradiance is increased, the deeper gratings form within a shorter time. However, at an irradiance of 521 mW/cm^2, the diffraction signal from azo glasses **4a-b** becomes more erratic, and the efficiencies decrease overall. Therefore, it can be concluded that the optimal irradiance for these samples is around 300 mW/cm^2, since the SRGs form quickly and exhibit high efficiency. On the other hand, compounds **4d-e** did not form any gratings at the aforementioned irradiances, even though the laser wavelength corresponds to the absorption maximum of compound **4d**. However, by increasing the irradiance of the laser to approximately 800 mW/cm^2, shallow SRGs with very low diffraction efficiencies appeared as seen in Figure 6. These gratings were barely visible to the naked eye. The

observed diffraction efficiency for compound **4e** was almost ten times smaller than that of compound **4d**, a consequence of its lower absorption at the incident wavelength. Longer irradiation times or higher irradiances resulted in the bleaching of the films, as well as a decrease in the diffraction efficiency.

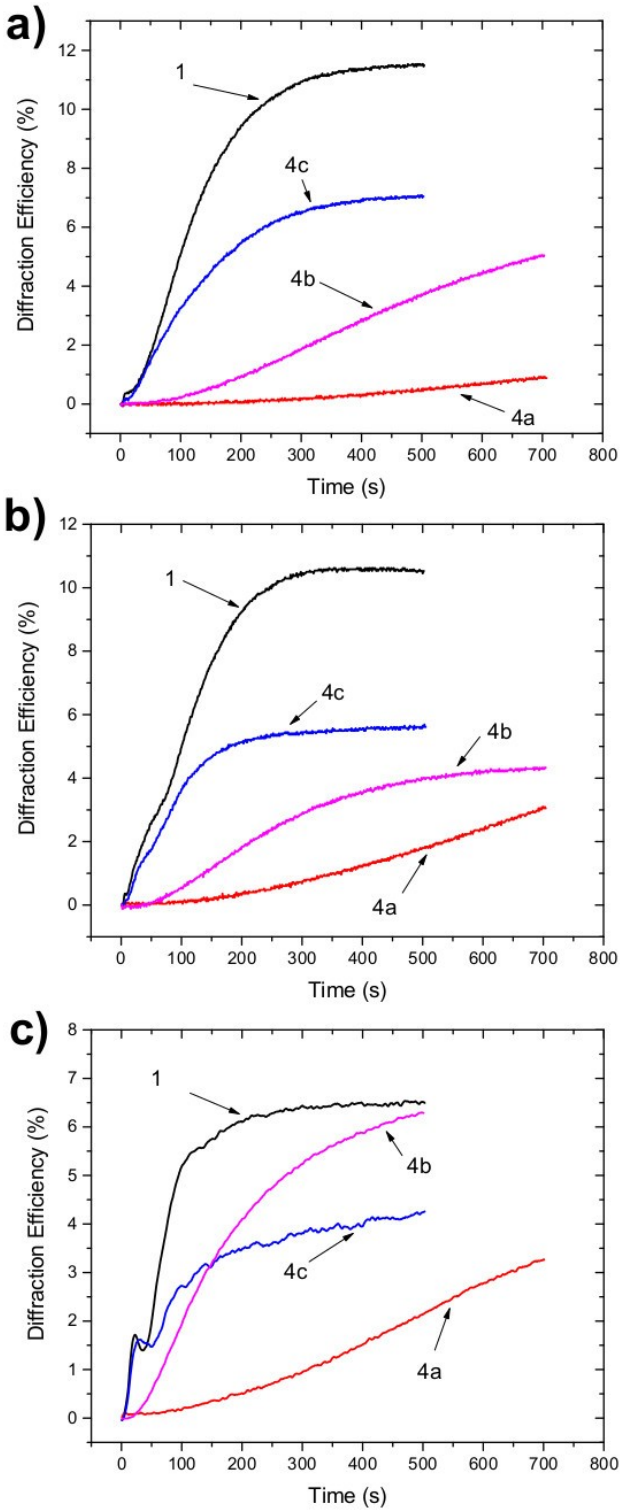

Fig. 5 Diffraction efficiency as a function of exposure time for films of azo glasses **1** and **4a-c** at the wavelength 532 nm and at the irradiances a) 157 mW/cm^2, b) 344 mW/cm^2, and c) 521 mW/cm^2.

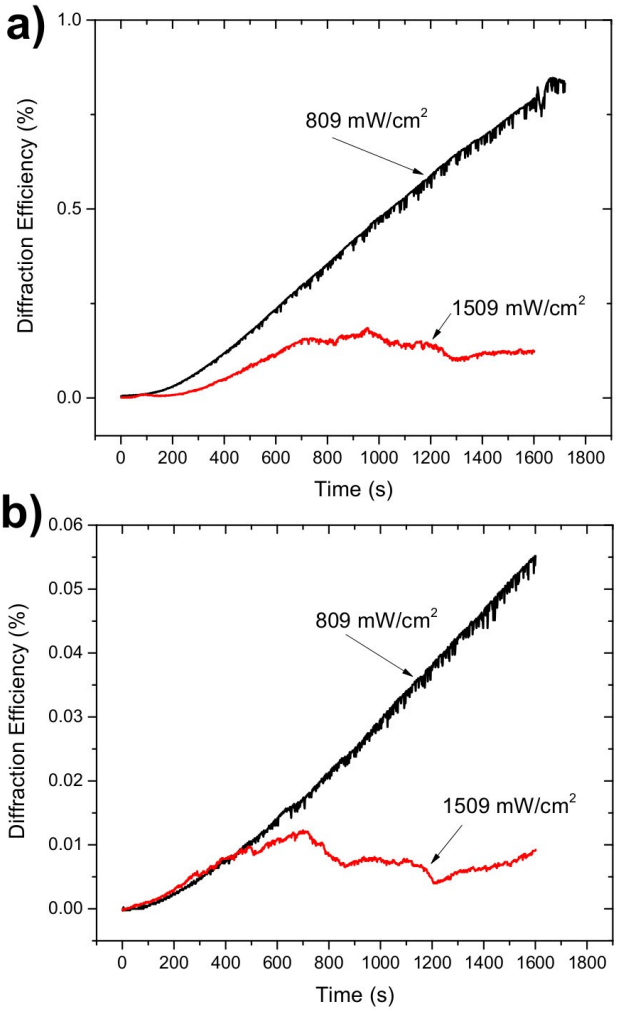

Fig. 6 Diffraction efficiency as a function of exposure time at the wavelength 532 nm and at irradiances of 809 or 1509 mW/cm^2 for films of azo glasses a) **4d**, and b) **4e**.

Finally, the diffraction efficiencies of the SRGs with the 632 nm He-Ne laser at an irradiance of 76 mW/cm^2 are shown in Figure 8. At this wavelength, only azo glasses **1** and **4c** form SRGs. However, the exposure time was much longer than with the other laser wavelengths. Arguably, the absorbance of compounds **4a-b** at this wavelength was too low to undergo isomerisation on the scale required for SRG formation, while in the case of compounds **4d-e**, a significantly higher irradiance would have been necessary for SRG growth.

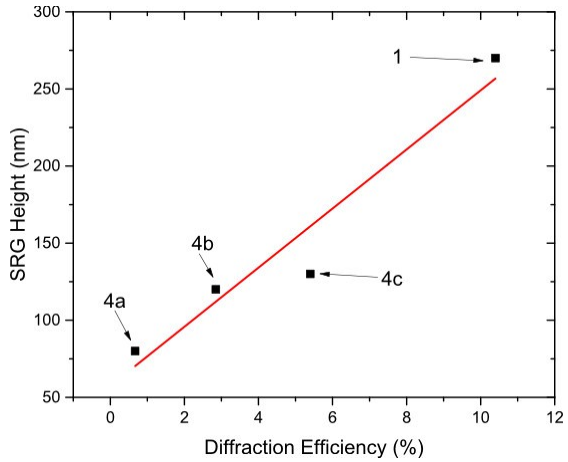

Fig. 7 SRG height as a function of diffraction efficiency for compounds **1** and **4a-c**. Heights were measured by AFM on SRG inscribed at the wavelength 532 nm with an irradiance of 344 mW/cm^2 and an exposure time of 300 s.

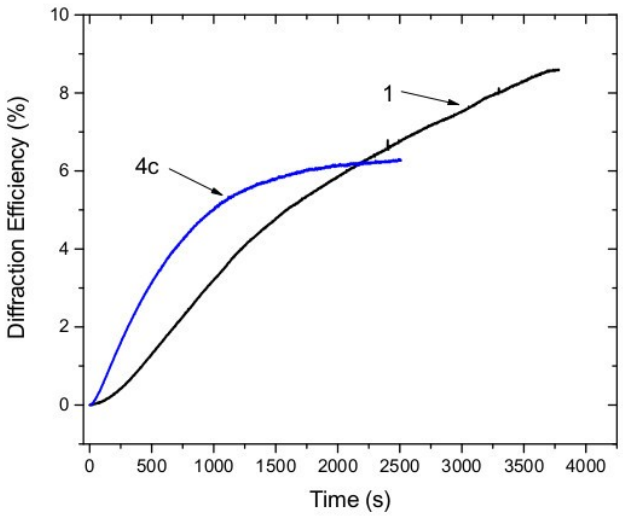

Fig. 8 Diffraction efficiency as a function of exposure time for films of azo glasses **1** and **4c** at the wavelength 632 nm and at an irradiance of 76 mW/cm^2.

These SRG inscription studies have shown that even though the absorbance of the chromophore at the wavelengths used impacts the rate of SRG formation, azo chromophores that absorb at lower wavelengths can form SRG more efficiently. This is likely due to the fact that rapid and continuous *cis-trans* isomerisation is required for the photomechanical effect responsible for SRG formation to occur,[37] and this isomerisation reaction is influenced by various parameters, including the activation energy and the *cis-trans* equilibrium constant. Photoisomerisation requires the absorption of photons to reach the excited state, but chromophores that undergo isomerisation with a higher quantum yield, faster kinetics, and with a non-negligible *cis* isomer population will form SRG with less overall absorption of light. On the other hand, the thiazole-containing chromophores of compounds **4d-e** show very weak SRG formation, even at wavelengths near the absorption maximum of compound **4d**.

The fact that azo chromophores bearing strongly electron-donating substituents on one ring and strongly electron-withdrawing substituents on the other (commonly referred to as the push-pull effect) show higher dipoles and higher stability of the *trans* isomer, has been well-documented.[31] Absorption maxima increase as a result of the stronger conjugation involving complementary substituents, which is accompanied by a strong dipole that stabilizes the *trans* isomer. The chromophore of compound **4d** has already been documented to exhibit low birefringence upon irradiation in the solid state, which is indicative of *cis-trans* isomerisation,[38] and to relax quickly to the *trans* isomer. It is unclear, however, if this behavior is due to the intrinsic high dipole of the chromophores, stronger aggregation of the azo moieties in the solid state, or even hydrogen bonding between thiazole nitrogen atoms and the triazine groups. Further studies are currently underway to investigate this behavior.

Conclusions

The strategy used to synthesize Disperse Red 1-functionalized glass **1** from Disperse Red 1 itself and a mexylaminotriazine precursor, which is simple and efficient, was used to generate a series of materials readily capable of forming stable glasses containing various similar azo chromophores with absorption maxima ranging from 410 to 570 nm. The compounds share very closely similar molecular structures, thereby allowing for a comparative study of the photomechanical properties of the various chromophores, in particular the inscription of surface relief gratings (SRG) and their relative rates of growth under irradiation with different wavelengths. Interestingly, for azobenzene chromophores, SRG formed even at wavelengths at which the compounds absorbed very weakly, whereas azothiazole chromophores showed very slow SRG growth even at wavelengths near their absorption maxima. The materials studied herein thus constitute an exciting family of azo materials that can readily form high-quality amorphous thin films with varying photophysical properties. While the azobenzene derivatives can form SRG, the Disperse Red 1 and azothiazole derivatives are used in nonlinear optics as a result of their strong dipoles.

Acknowledgements

The authors would like to thank the Academic Research Programme (ARP) of RMC and the Discovery Grants Program from the Natural Sciences and Engineering Research Council (NSERC #327116) for funding. The authors would also like to thank Dr. René Gagnon (Université de Sherbrooke) for mass spectrometry analyses, Dr. Hirohito Umezawa (Fukushima National College of Technology) for acquisition of some AFM scans, as well as Dr. Paul Rochon (Royal Military College of Canada) for useful discussions.

Notes and references

[a] *Department of Chemistry, Department of Physics, Queen's University,*

Kingston, K7L 3N6, Canada. Fax: +1 613-533-6669; Tel: +1 613-533-6749; E-mail: nunzijm@queensu.ca
[b] *Department of Physics, Royal Military College of Canada, Kingston, ON, K7K 7B4, Canada. Fax: +1 613-541-6040; Tel: +1 613-6541-6000 ext. 6721; E-mail: sabat@rmc.ca*
[c] *Department of Chemistry and Chemical Engineering, Royal Military College of Canada, Kingston, ON, K7K 7B4, Canada. Fax: +1 613-542-9489; Tel: +1 613-541-6000 ext. 3694; E-mail: Olivier.Lebel@rmc.ca*
† Electronic Supplementary Information (ESI) available: Synthetic procedures and spectral data for compounds **4b-4e**, additional data on SRG growth for compounds **1** and **4a-4e**, NMR spectra for compounds **4a-e**. See DOI: 10.1039/b000000x/
‡ Marvin was used for drawing, displaying and characterizing chemical structures, substructures and reactions, Marvin 15.1.12, 2015, ChemAxon (http://www.chemaxon.com).

1 Z. Sekkat and W. Knoll (Editors), *Photoreactive Organic Thin Films*, Academic Press, Amsterdam, 2002.
2 C. Cojocariu and P. Rochon, *Pure Appl. Chem.*, 2004, **76**, 1479-1497.
3 N.K. Viswanathan, D.Y. Kim, S. Bian, J. Williams, W. Liu, L. Li, L. Samuelson, J. Kumar and S.K. Tripathy, *J. Mater. Chem.*, 1999, **9**, 1941-1955.
4 A. Priimagi and A. Shevchenko, *J. Polym. Sci., Part B: Polym. Phys.*, 2014, **52**, 163-182.
5 P. Rochon, E. Batalla and A. Natansohn, *Appl. Phys. Lett.*, 1995, **66**, 136-138.
6 R.J. Stockermans and P.L. Rochon, *Appl. Opt.*, 1999, **38**, 3714-3719.
7 J.P. Monteiro, J. Ferreira, R.G. Sabat, P. Rochon, M.J.L. Santos and E.M. Girotto, *Sensors Actuators B: Chem.*, 2012, **174**, 270-273.
8 T. Chida and Y. Kawabe, *Opt. Mater.*, 2014, **36**, 778-781.
9 C. Hubert, C. Fiorini-Debuisschert, I. Hassiaoui, L. Rocha, P. Raimond and J.-M. Nunzi, *Appl. Phys. Lett.*, 2005, **87**, 191105.
10 J. Jefferies and R.G. Sabat, *Prog. Photovolt:Res. Appl.*, 2012, DOI: 10.1002/pip.2326.
11 C. Cocoyer, L. Rocha, L. Sicot, B. Geffroy, R. de Bettignies, C. Sentein, C. Fiorini-Debuisschert and P. Raimond, *Appl. Phys. Lett.*, 2006, **88**, 133108.
12 Z. Mahimwalla, K.G. Yager, J.-I. Mamiya, A. Shishido, A. Priimagi and C.J. Barrett, *Polym. Bull.*, 2012, **69**, 967-1006.
13 A. Natansohn and P. Rochon, *Adv. Mater.*, 1999, **11**, 1387-1391.
14 A. Natansohn and P. Rochon, *Chem. Rev.*, 2002, **102**, 4139-4175.
15 H. Nakano, T. Takahashi, T. Kadota and Y. Shirota, *Adv. Mater.*, 2002, **14**, 1157-1160.
16 E. Ishow, B. Lebon, Y. He, X. Wang, L. Bouteiller, L. Galmiche and K. Nakatani, *Chem. Mater.*, 2006, **18**, 1261-1267.
17 K. Traskovskis, I. Mihailovs, A. Tokmakovs, A. Jurgis, V. Kokars and M. Rutkis, *J. Mater. Chem.*, 2012, **22**, 11268-11276.
18 C.A. Angell, *Science*, 1995, **267**, 1924-1935.
19 M.D. Ediger, C.A. Angell and S.R. Nagel, *J. Phys. Chem.*, 1996, **100**, 13200-13212.
20 Y. Shirota, *J. Mater. Chem.*, 2000, **10**, 1-25.
21 P. Strohriegl and J.V. Grazulevicius, *Adv. Mater.*, 2002, **14**, 1439-1452.
22 Y. Shirota and H. Kageyama, *Chem. Rev.*, 2007, **107**, 953-1010.
23 R. Lygaitis, V. Getautis and J.V. Grazulevicius, *Chem. Soc. Rev.*, 2008, **37**, 770-788.
24 O. Lebel, T. Maris, M.-È. Perron, E. Demers and J.D. Wuest, *J. Am. Chem. Soc.*, 2006, **128**, 10372-10373.
25 A. Plante, D. Mauran, S.P. Carvalho, J.Y.S.D. Pagé, C. Pellerin and O. Lebel, *J. Phys. Chem. B*, 2009, **113**, 14884-14891.
26 R.N. Eren, A. Plante, A. Meunier, A. Laventure, Y. Huang, J.G. Briard, K.J. Creber, C. Pellerin, A. Soldera and O. Lebel, *Tetrahedron*, 2012, **68**, 10130-10144.
27 A. Meunier and O. Lebel, *Org. Lett.*, 2010, **12**, 1896-1899.
28 F. Borbone, A. Carella, L Ricciotti, A. Tuzi, A. Roviello and A. Barsella, *Dyes Pigments*, 2011, **88**, 290-295.
29 C. Barrett, A. Natansohn and P. Rochon, *Chem. Mater.*, 1995, **7**, 899-903.
30 Z.-S. Xu, A. Natansohn and P. Rochon, *J. Macromol. Sci., Pure Appl. Chem.*, 2001, **A38**, 1305-1314
31 C. Cojocariu and P. Rochon, *J. Mater. Chem.*, 2004, **14**, 2909-2016.
32 R. Kirby, R.G. Sabat, J.-M. Nunzi and O. Lebel, *J. Mater. Chem. C*, 2014, **2**, 841-847.
33 C. Vijayakumar, B. Balan, M.-J. Kim and M. Takeuchi, *J. Phys, Chem. C*, 2011, **115**, 4533-4539.
34 F. De Feo, S. Papa and E. Traverso, US Pat. Appl. YS 4011209 A, 1977.
35 L. Chen, Y. Cui, G. Qian and M. Wang, *Dyes Pigments*, 2007, **73**, 338-343.
36 Y. Cui, G. Qian, L. Chen, Z. Wang and M. Wang, *Dyes Pigments*, 2008, **77**, 217-222.
37 A. Natansohn, S. Xie and P. Rochon, *Macromolecules*, 1992, **25**, 5531-5532.
38 P. Rochon, J. Gosselin, A. Natansohn and S. Xie, *Appl. Phys. Lett.*, 1992, **60**, 4.